

A central arteriovenous fistula reduces systemic hypertension in a mouse model



Anand Brahmandam, MD,^{a,b} Rafael Alves, BM,^a Hao Liu (刘灏), MD,^{a,c} Luis Gonzalez, PhD,^a Yukihiro Aoyagi (青柳 幸彦), MD,^{a,d} Yuichi Ohashi (大橋 雄一), MD,^{a,e} John T. Langford, MD,^a Carly Thaxton, MD,^a Ryosuke Taniguchi (谷口 良輔), MD, PhD,^{a,e} Weichang Zhang (张惟常), MD, PhD,^a Hualong Bai (白华 龙), MD, PhD,^a Bogdan Yatsula, PhD,^a and Alan Dardik, MD, PhD,^{a,b,f,g} *New Haven and West Haven, CT; Guangzhou, China; and Fukuoka and Tokyo, Japan*

ABSTRACT

Objective: A central arteriovenous fistula (AVF) has been proposed as a potential novel solution to treat patients with refractory hypertension. We hypothesized that venous remodeling after AVF creation in the hypertensive environment reduces systemic blood pressure but results in increased AVF wall thickness compared with remodeling in the normotensive environment.

Methods: A central AVF was performed in C57BL6/J mice previously made hypertensive with angiotensin II (Ang II); mice were sacrificed on postoperative day 7 or 21.

Results: In mice treated with Ang II alone, the mean systolic blood pressure increased from 90 ± 5 mmHg to 160 ± 5 mmHg at day 21; however, in mice treated with both Ang II and an AVF, the blood pressure decreased with creation of an AVF. There were significantly more PCNA-positive cells, SM22 α /PCNA-positive cells, collagen I deposition, and increased Krüppel-like Factor 2 immunoreactivity in hypertensive mice with an AVF compared with normotensive mice with an AVF.

Conclusions: These data show that a central AVF decreases systemic hypertension as well as induces local alterations in venous remodeling. (*JVS—Vascular Science* 2024;5:100191.)

Keywords: Angiotensin II; Arteriovenous fistula; Hypertension; Neointimal hyperplasia

Nearly one-half the adult population in the United States has hypertension, but only one-half of these patients have adequate control,¹ resulting in excess morbidity and health care costs of approximately \$131 billion each year.^{2,3} Uncontrolled hypertension is associated with a significantly increased risk for stroke, atherosclerosis, aortic aneurysm, dissection, and hypertensive nephropathy.¹

A central arteriovenous fistula (AVF) has been proposed as a potential novel solution for hypertension; creation of an AVF significantly decreases blood pressure, and subsequent AVF ligation increases blood pressure.⁴⁻⁶ Creation of a central iliac AVF reduces both systolic and diastolic blood pressure by approximately 20 to 25 mmHg⁵; the central AVF is associated with significantly fewer hypertensive complications, suggesting its

use as an adjunctive therapy for patients with refractory hypertension.⁷

Hemodynamics play a complex role during AVF maturation,⁸ resulting in vessel remodeling that leads to dilation, smooth muscle cell (SMC) proliferation and wall thickening, and potentially neointimal hyperplasia.⁹⁻¹¹ Most studies of vessel remodeling after AVF creation examine the changes resulting from exposure to physiological arterial flow and pressure; however, the influence of hypertension on AVF maturation and remodeling is not well understood. We hypothesize that venous remodeling after AVF creation in the hypertensive environment reduces systemic blood pressure but results in increased wall thickening compared with remodeling in the normotensive environment. We tested our hypothesis using an established mouse central AVF model

From the Vascular Biology and Therapeutics Program, Yale School of Medicine^a; and the Division of Vascular Surgery and Endovascular Therapy, Department of Surgery, Yale School of Medicine,^b New Haven; the Division of Vascular and Interventional Radiology, Department of General Surgery, Nanfang Hospital, Southern Medical University, Guangzhou^c; the Department of Surgery and Science, Graduate School of Medical Sciences, Kyushu University, Fukuoka^d; the Division of Vascular Surgery, Department of Surgery, The University of Tokyo, Tokyo^e; the Department of Cellular and Molecular Physiology, Yale School of Medicine, New Haven^f; and the Surgical Service, VA Connecticut Healthcare System, West Haven.^g

This study was supported by the National Institutes of Health Grants R01-HL144476 and R01-HL162580, and the resources and use of facilities at the Veterans Affairs Connecticut Healthcare System (West Haven, CT).

AB and RA contributed equally to this article and share co-first authorship.

Correspondence: Alan Dardik, MD, PhD, Yale School of Medicine, 10 Amistad Street, Room 437, PO Box 208089, New Haven, CT 06520-8089 (e-mail: alan.dardik@yale.edu).

The editors and reviewers of this article have no relevant financial relationships to disclose per the Journal policy that requires reviewers to decline review of any manuscript for which they may have a conflict of interest.

2666-3503

Published by Elsevier Inc. on behalf of the Society for Vascular Surgery. This is an open access article under the CC BY-NC-ND license (<http://creativecommons.org/licenses/by-nc-nd/4.0/>).
<https://doi.org/10.1016/j.jvssci.2024.100191>

coupled with the angiotensin II (Ang II) hypertensive model.¹²

METHODS

Murine hypertension model and aortocaval arteriovenous fistula. All murine experiments were performed in strict compliance with Federal recommendations and approval from the Yale University Institutional Animal Care and Use Committee. Wild-type male C57BL6/J mice 9 to 11 weeks of age were used in this study; female mice were not used due to sex differences in hemodynamics in this AVF model,^{8,13} as well as variations in the blood pressure after Ang II infusion.¹⁴ Noninvasive blood pressure measurements were performed using the tail-cuff method (CODA System; Kent Scientific) as previously described,¹⁵ with all measurements performed at the same time of day.

An Ang II infusion pump (500 ng/kg/min; Sigma-Aldrich) was used to induce hypertension as previously described.¹² Anesthesia was administered using 2% to 2.5% isoflurane, and postoperative pain control was provided for 48 hours after surgery with buprenorphine (0.1 mg/kg, intraperitoneally). An osmotic pump (model 2004; Alzet) was implanted in a subcutaneous tunnel over the back (Fig 1, A). An AVF was created at day 14 after osmotic pump implantation as previously described.¹⁰

Mice were randomly divided into four groups (Fig 1, A): control (vehicle: saline-filled osmotic pump implantation with sham surgery), hypertension (Ang II pump implantation with sham surgery), AVF (vehicle: saline-filled osmotic pump implantation with AVF surgery), and hypertension and AVF (Ang II pump implantation with AVF surgery). Doppler ultrasound examination (Vevo 770 High-Resolution Imaging System, Fujifilm Visual Sonics Inc) was used to examine the AVF serially in vivo (Fig 1, A). Blood flow, shear stress, and time-averaged mean velocity were calculated using the Hagen-Poiseuille formula (Fig 1, B). The viscosity of blood was assumed to be constant at 0.0035 Poise. Mouse AVF samples were harvested on postoperative days 0, 7, or 21 after flushing with cold normal saline followed by 10% formalin solution via the left ventricle under physiologic pressure.

Histology. This tissue was embedded in paraffin and sectioned (5- μ m thickness). Cross-sections were obtained 50 to 100 μ m cranial to the AVF.¹⁰ Hematoxylin and eosin, Elastin Van Gieson, and Masson's trichrome staining were performed. Digital images were captured using a light microscope (BX40; Q-Color 5, Olympus America). Neointimal thickness and collagen area were measured using ImageJ software (National Institutes of Health) as previously described.^{9,16}

Immunofluorescence. Sections were deparaffined using xylene and rehydrated in a graded series of alcohol.

ARTICLE HIGHLIGHTS

- **Type of Research:** Mouse model of systemic hypertension and central arteriovenous fistula (AVF)
- **Key Findings:** In a mouse model of hypertension, a central AVF reduces systemic blood pressure. There were significantly more PCNA-positive cells, SM22 α /PCNA-positive cells, and collagen I deposition, suggestive of smooth muscle cell proliferation and increased Krüppel-like Factor 2 immunoreactivity in hypertensive mice with an AVF compared with normotensive mice with an AVF.
- **Take Home Message:** A mouse model shows that a central AVF treats hypertension, similar to human patients. Hypertension alters the adaptive venous remodeling that may affect AVF maturation.

The sections were then heated for 10 minutes for antigen retrieval in a citric acid buffer (pH 6.0, 100 °C); sections were then blocked with 2% bovine serum albumin in phosphate-buffered saline containing 0.1% Tween20 for 1 hour at room temperature. Following this, the sections were incubated overnight at 4 °C with the primary antibodies (Table) diluted in 2% bovine serum albumin. The sections were then treated with appropriate secondary antibodies (Table) at room temperature for 1 hour; the sections were then stained with 4'6-diamidino-2-phenylindole (P36935; Invitrogen), and a coverslip was applied. Digital fluorescence images were captured using the Invitrogen EVOS M7000 Imaging System, and the intensity of the immunoreactive signal was measured using ImageJ software (National Institutes of Health).

Statistical analysis. Normality of samples was tested using the Shapiro-Wilk test, and the *F* test was performed to evaluate homogeneity of variances. The cohorts were then compared using one-way analysis of variance (ANOVA), or mixed effects analysis with post hoc testing using Tukey's multiple comparisons test for multiple group comparisons for normally distributed data. For comparisons involving two factors, two-way ANOVA with post hoc testing using Tukey's multiple comparisons test was used. For multiple group comparisons with lognormal distribution, the Kruskal-Wallis test was used. Statistical significance was set at $P < .05$. All statistical analyses were performed using Prism 9 (Prism, Graph Pad, Inc).

RESULTS

To determine the effects of an AVF in wild-type male mice with hypertension, we implanted osmotic pumps that continuously released Ang II or a vehicle 2 weeks prior to AVF creation (Fig 1, A).¹² In control mice without Ang II, the blood pressure did not significantly change over time either in the absence (Fig 2, A, open circles)

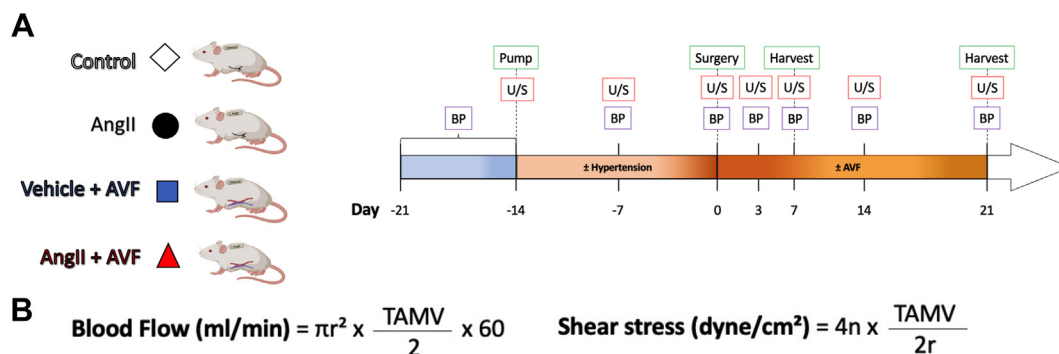


Fig 1. Experimental design. **A**, Diagram showing experimental groups and timeline: control (white diamond), angiotensin II (Ang II) (black circle), vehicle + arteriovenous fistula (AVF) (blue square), and Ang II + AVF (red triangle). Day 0, AVF creation. Light blue, Pre-hypertension phase (1 week prior to pump implantation); orange, induction of hypertension (14 days prior to AVF creation); yellow, vascular remodeling phase after AVF creation, without or with hypertension. Mice were harvested at 7 or 21 days after AVF creation. Ultrasound (U/S) and blood pressure (BP) were measured at days 0, 3, 7, 14, and 21 immediately prior to harvest. **B**, Equations to calculate hemodynamics. TAMV, Time-averaged mean velocity.

Table. Primary and secondary antibodies used in this research

Antibody	Vendor	Lot number	Concentration
Primary antibody			
Anti-goat SM22 alpha	Abcam	ab10135	1:200
Anti-goat CD31	R&D	AF3628	1:200
Anti-rabbit PCNA	Abcam	ab92552	1:50
Anti-rabbit Collagen I	Abcam	ab34710	1:50
Anti-rabbit NF-κB p65	Abcam	ab16502	1:50
Anti-rabbit KLF2	LSBio	B5627	1:50
Secondary antibody			
Anti-goat Alexa Fluor 458	Invitrogen	A11055	1:500
Anti-rabbit Alexa Fluor 647	Invitrogen	A21443	1:500

or the presence of an AVF (Fig 2, A, blue line). In mice treated with Ang II alone, the mean systolic blood pressure increased gradually from a baseline of 90 ± 5 mmHg to a peak of 160 ± 5 mmHg at day 21 (Fig 2, A, black line); however, in mice treated with both Ang II and an AVF, the blood pressure did not rise after AVF creation (Fig 2, A, red line). These data show that the creation of a central AVF reduces the systemic blood pressure in the Ang II environment.

Measurement of hemodynamics in the inferior vena cava (IVC) cranial to the AVF showed a significantly increased IVC diameter in mice with an AVF (Fig 2, B, blue and red lines) compared with mice without an AVF (Fig 2, B, black line). Immediately after Ang II osmotic pump implantation, there was no difference in peak systolic velocity (PSV), shear stress, or blood flow between the groups. However, after AVF creation (Fig 2, C-E), there

was significantly increased PSV, shear stress, and blood flow in mice treated with an AVF and Ang II (Fig 2, C-E, red lines) compared with mice treated with an AVF and vehicle alone (Fig 2, C-E, blue lines). These changes suggest that the presence of an AVF in a hypertensive environment significantly alters the hemodynamics in the outflow IVC compared with normotensive mice.

The IVC wall was significantly thicker in mice with an AVF compared with mice without AVF (Fig 2, F; blue vs white bars), and mice with both AVF and Ang II treatment had even thicker walls at both day 7 and day 21 (Fig 2, F-C; red vs black bars). Similarly, there were significantly more SM22 α -positive cells in the IVC wall in mice with an AVF, and mice with both an AVF and Ang II treatment had significantly greater numbers of SM22 α -positive cells at both day 7 and day 21 (Fig 2, H-I). There were also increased percent of PCNA-positive cells in mice with both an AVF and Ang II treatment (Fig 3, A-B), consistent with increased cell proliferation, as well as increased percent of SM22 α /PCNA-positive cells in mice with both an AVF and Ang II treatment (Fig 3, C-D). There was no increase in cleaved caspase-3 positive cells in any group (Fig 3, E-F). These data show differential venous remodeling of the AVF in the Ang II environment compared with the normotensive environment, with cell turnover in the AVF wall driven by cell proliferation.

Because wall thickening may also be due to increased amounts of extracellular matrix components,¹¹ we examined the AVF wall for collagen; there was significantly increased collagen in mice with an AVF compared with mice without an AVF, and mice with both an AVF and Ang II treatment had even greater collagen area at both day 7 and day 21 (Fig 4, A-B). Similarly, there was significantly increased collagen-1 immunoreactivity in mice with an AVF compared with mice without an

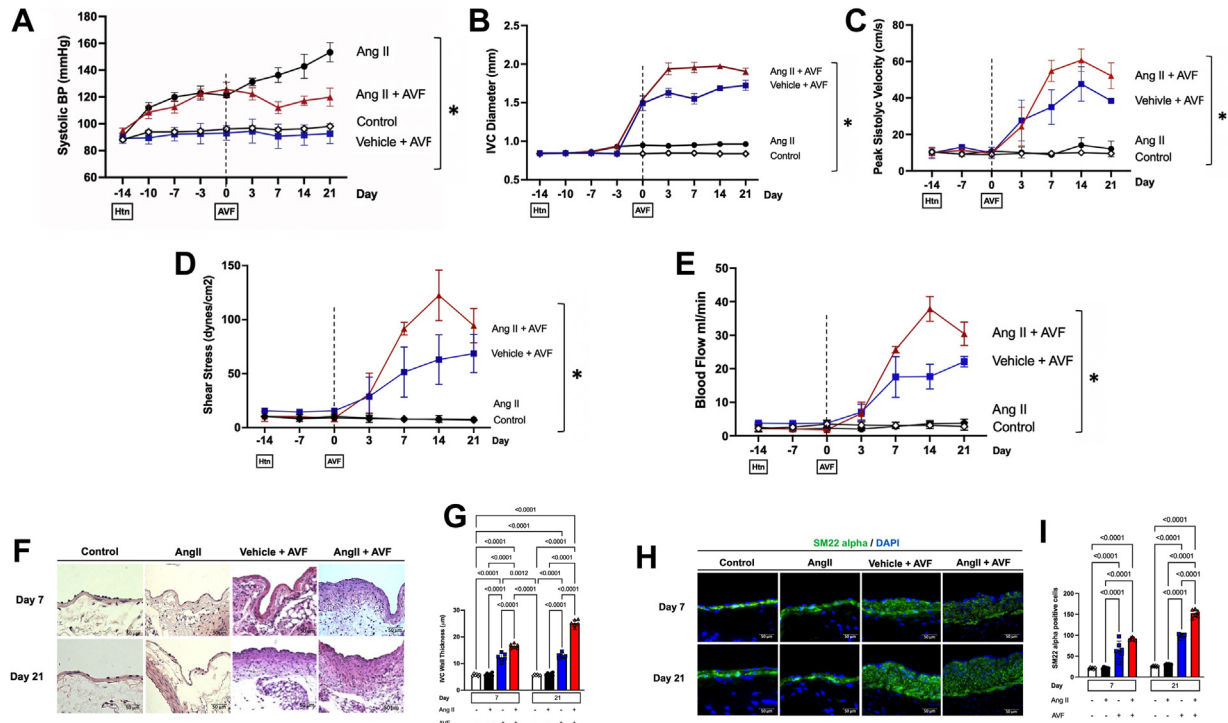


Fig 2. Hemodynamic and morphological changes in the arteriovenous fistula (AVF) without or with hypertension. **A**, Blood pressure (BP) (mmHg) in the control (white), angiotensin II (Ang II) (black), vehicle + AVF (blue), and Ang II + AVF (red) groups; $*P \leq .0001$ (two-way analysis of variance [ANOVA]); $n = 5$. Difference between Ang II vs Ang II AVF groups, $P = .0376$ (Tukey's multiple comparisons test). **B**, Inferior vena cava (IVC) diameter in the control (white), Ang II (black), vehicle + AVF (blue), and Ang II + AVF (red) groups; $*P \leq .0001$ (two-way ANOVA); $n = 11-13$. Difference between Ang II vs Ang II AVF groups, $P \leq .0001$ (Tukey's multiple comparisons test). **C**, Peak systolic velocity (PSV) in the control (white), Ang II (black), vehicle + AVF (blue), and Ang II + AVF (red) groups; $*P \leq .0001$ (two-way ANOVA); $n = 3$. Difference between Ang II vs Ang II AVF groups, $P = .0421$ (Tukey's multiple comparisons test). **D**, Shear stress in the control (white), Ang II (black), vehicle + AVF (blue), and Ang II + AVF (red) groups, $P \leq .0001$ (two-way ANOVA); $n = 3$. Difference between Ang II vs Ang II AVF groups, $P = .0248$ (Tukey's multiple comparisons test). **E**, Blood flow in the control (white), Ang II (black), vehicle + AVF (blue), and Ang II + AVF (red) groups; $*P \leq .0001$ (two-way ANOVA); $n = 3$. Difference between Ang II vs Ang II AVF groups, $P = .0284$ (Tukey's multiple comparisons test). **F**, Hematoxylin and eosin (H&E) staining of the IVC wall in the control (first column), Ang II (second column), vehicle + AVF (third column), and Ang II + AVF groups (fourth column), at day 7 (first row) or 21 (second row); scale bar, 50 μm ; $n = 6$. **G**, Bar graph showing IVC wall thickness in the control (white), Ang II (black), AVF (blue), and Ang II + AVF (red) groups at days 7 and 21; $P \leq .0001$ (two-way ANOVA); values of Tukey's multiple comparisons test are shown; $n = 6$. **H**, Merged immunofluorescence showing SM22 alpha (green) and DAPI (blue) in the control (first column), Ang II (second column), vehicle + AVF (third column), and Ang II + AVF groups (fourth column), at day 7 (first row) or 21 (second row); scale bar, 50 μm ; $n = 6$. **I**, Bar graph showing the number of SM22 positive cells in the control (white), Ang II (black), AVF (blue), and Ang II + AVF (red) groups at days 7 or 21; $P \leq .001$ (two-way ANOVA); values of Tukey's multiple comparisons test are shown; $n = 6$.

AVF, and mice with both an AVF and Ang II treatment had greater collagen-1 immunoreactivity at both day 7 and day 21. These data support that the creation of an AVF in a hypertensive environment results in increased collagen deposition in the AVF wall.

Because our data show hemodynamic changes in AVF in the Ang II environment (Fig 2), we examined the expression of Krüppel-like Factor 2 (KLF2) and nuclear factor kappa beta (NF κ B) in the AVF wall.^{17,18} In mice with an AVF, KLF2 immunoreactivity decreased significantly compared with mice without an AVF, consistent with our previous data¹⁹; interestingly, there was

increased KLF2 immunoreactivity in mice treated with both an AVF and Ang II (Fig 5, A-B). Similarly, NF κ B immunoreactivity decreased in mice treated with an AVF, and additionally decreased in mice additionally treated with Ang II (Fig 5, C-D). These data suggest that KLF2 and NF κ B immunoreactivity are reciprocally altered concordant with the hemodynamic changes in the remodeling AVF in the Ang II environment.

DISCUSSION

We show that a central AVF decreases hypertension in hypertensive mice (Fig 2), and is associated with

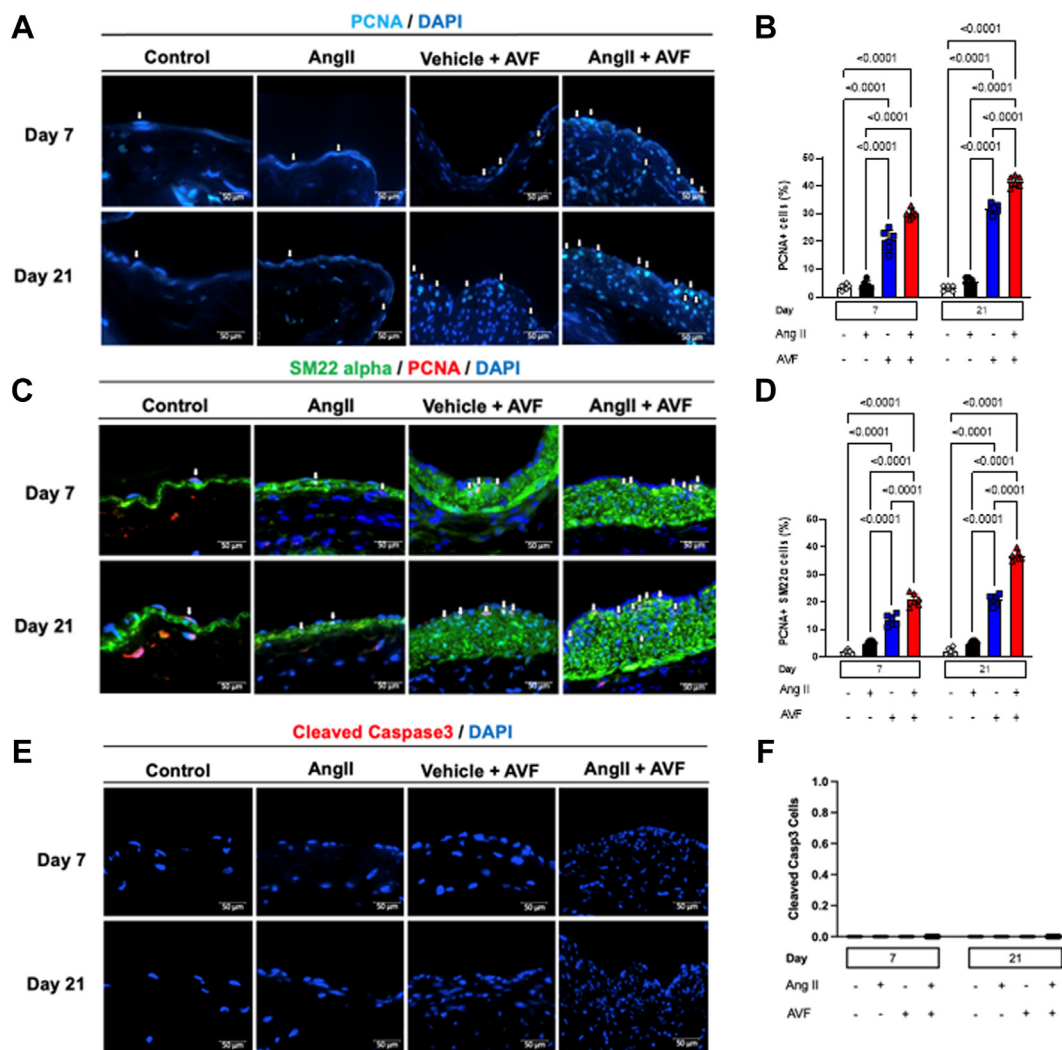


Fig 3. Neointimal cell turnover in the arteriovenous fistula (AVF) without or with hypertension. **A**, Merged immunofluorescence showing PCNA (light blue) and DAPI (dark blue), in the control (first column), angiotensin II (Ang II) (second column), vehicle + AVF (third column), and Ang II + AVF groups (fourth column), at day 7 (first row) or 21 (second row); scale bar, 50 μ m; $n = 6$; white arrows show the PCNA-positive cells. **B**, Bar graph showing the percentage of PCNA-positive cells; $P \leq .001$ (two-way analysis of variance [ANOVA]); values of Tukey's multiple comparisons test are shown; $n = 6$. **C**, Merged immunofluorescence showing SM22 alpha (green), PCNA (red), and DAPI (blue) in the control (first column), Ang II (second column), vehicle + AVF (third column), and Ang II + AVF groups (fourth column), at day 7 (first row) or 21 (second row); scale bar, 50 μ m or 100 μ m; $n = 6$; white arrows show the PCNA- and SM22 alpha-dual positive cells. **D**, Bar graph showing the percentage of PCNA- and SM22 alpha-dual positive cells; $P \leq .001$ (two-way ANOVA); values of Tukey's multiple comparisons test are shown; $n = 6$. **E**, Merged immunofluorescence showing cleaved caspase-3 (Casp3, red) and DAPI (blue) in the control (first column), Ang II (second column), vehicle + AVF (third column), and Ang II + AVF groups (fourth column), at day 7 (first row) or 21 (second row); scale bar, 50 μ m; $n = 6$. **F**, Bar graph showing the number of cleaved caspase3 (Casp3)-positive cells; $P = 1.000$ (two-way ANOVA); $n = 6$.

increased AVF wall thickness (Fig 2), SMC proliferation (Fig 3), and collagen deposition (Fig 4). These data show that this mouse model recapitulates similar results in human patients and also show that hypertension has effects on the remodeling AVF wall.

The prevalence of drug-resistant hypertension varies among different studies, from less than 10% to 20%; drug-resistant hypertension carries a 25% higher risk of stroke over a 5-year period compared with patients

without resistant hypertension.^{5,20} New research has suggested the use of an AVF as a potential treatment for hypertension, such as the ROX coupler that creates an iliac AVF.⁶ In hypertensive patients treated with a ROX coupler, the mean office systolic blood pressure was reduced by 26.9 ± 23.9 mmHg, and the mean systolic 24-hour ambulatory blood pressure was reduced by 13.5 ± 18.8 mmHg.⁵ Ott et al showed efficacy of the ROX coupler in both isolated systolic hypertension

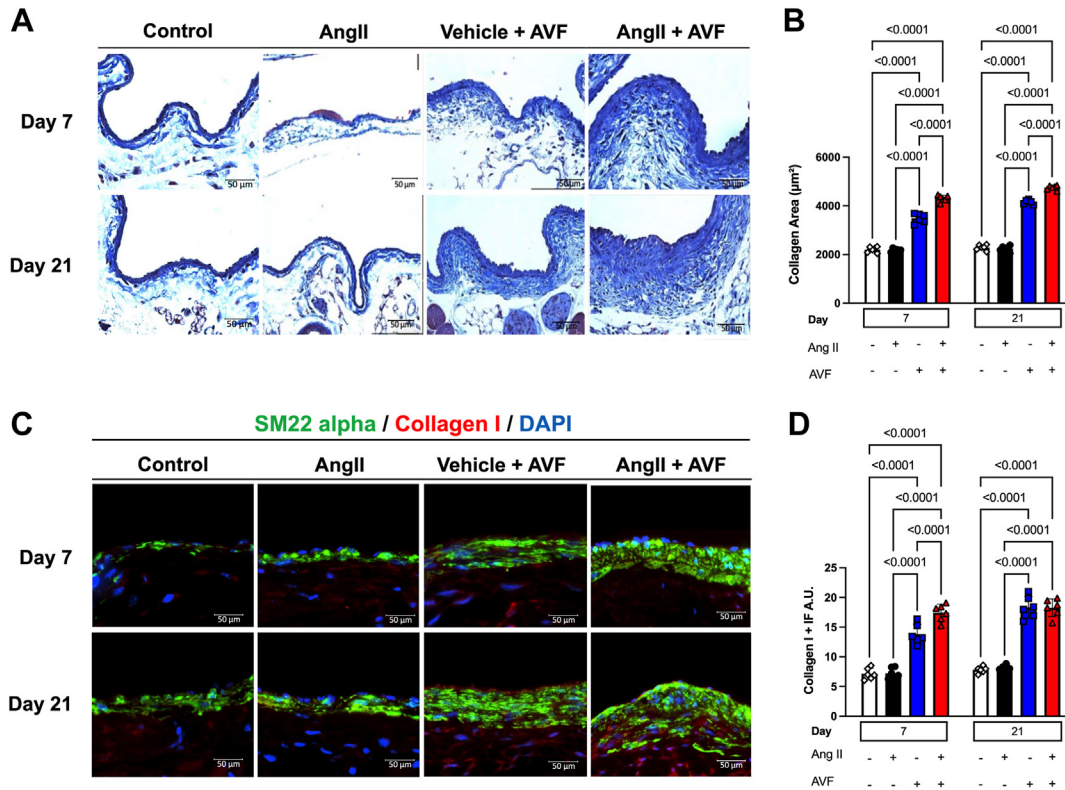


Fig 4. Collagen deposition in the arteriovenous fistula (AVF) without or with hypertension. **A**, Masson's Trichrome staining in the control (first column), angiotensin II (Ang II) (second column), vehicle + AVF (third column), and Ang II + AVF groups (fourth column), at day 7 (first row) or 21 (second row); scale bar, 50 µm; n = 6. **B**, Bar graph showing the mean collagen area; $P \leq .001$ (two-way analysis of variance [ANOVA]); values of Tukey's multiple comparisons test are shown; n = 6. **C**, Merged immunofluorescence showing SM22 alpha (green), collagen I (red), and DAPI (blue) in the control (first column), Ang II (second column), vehicle + AVF (third column), and Ang II + AVF groups (fourth column), at day 7 (first row) or 21 (second row); scale bar, 50 µm; n = 6. **D**, Bar graph showing mean collagen I fluorescence intensity; $P \leq .001$ (two-way ANOVA); values of Tukey's multiple comparisons test are shown; n = 6.

and combined hypertension.⁴ Our data is consistent with this effect, with $15\% \pm 2\%$ reduction in blood pressure in the presence of an AVF (Fig 2). Furthermore, this data is consistent with our previous data showing potential cardiac-protective effects of an AVF.²¹ Together these data suggest the beneficial effect of a central AVF to lower the blood pressure in resistant hypertension, as well as induce protective cardiac remodeling.

The correlation between hypertension and AVF maturation remains unclear. There is an increased number of proliferating vascular SMC in hypertensive patients,²² similar to our data (Fig 3). Because neointimal SMC proliferation contributes to long-term AVF failure,²³ hypertension might negatively influence long-term AVF patency. In addition, collagen deposition in the cardiovascular system can increase stiffness and may also be influenced by hypertension.²⁴⁻²⁷ We previously showed that extracellular matrix components have a distinct temporal pattern of expression in this model,²⁸ and there is significantly more and earlier collagen deposition in

hypertensive mice compared with normotensive mice (Fig 4), consistent with a negative influence on venous remodeling with hypertension. On the other hand, several studies have reported an association of hypertension with higher rates of successful AVF maturation.²⁹⁻³² In these cases, increased SMC number and collagen deposition could increase wall strength and contribute to improved AVF maturation. These seemingly paradoxical influences of hypertension on AVF maturation and long-term patency, and whether anti-hypertensive therapy has an effect on AVF maturation, require further investigation.

Endothelial cells acquire atheroprotective or atherogenic phenotypes when exposed to laminar or disturbed flow, respectively.³³⁻³⁵ In this mouse AVF model, turbulent flow decreases KLF2 expression.¹⁹ In a rat carotid-jugular AVF model, alteration of fistula geometry using the artery to vein configuration is associated with increased expression of KLF2 and phosphorylated endothelial nitric oxide synthase (eNOS) compared with expression in AVF with conventional vein to artery geometry, suggesting that

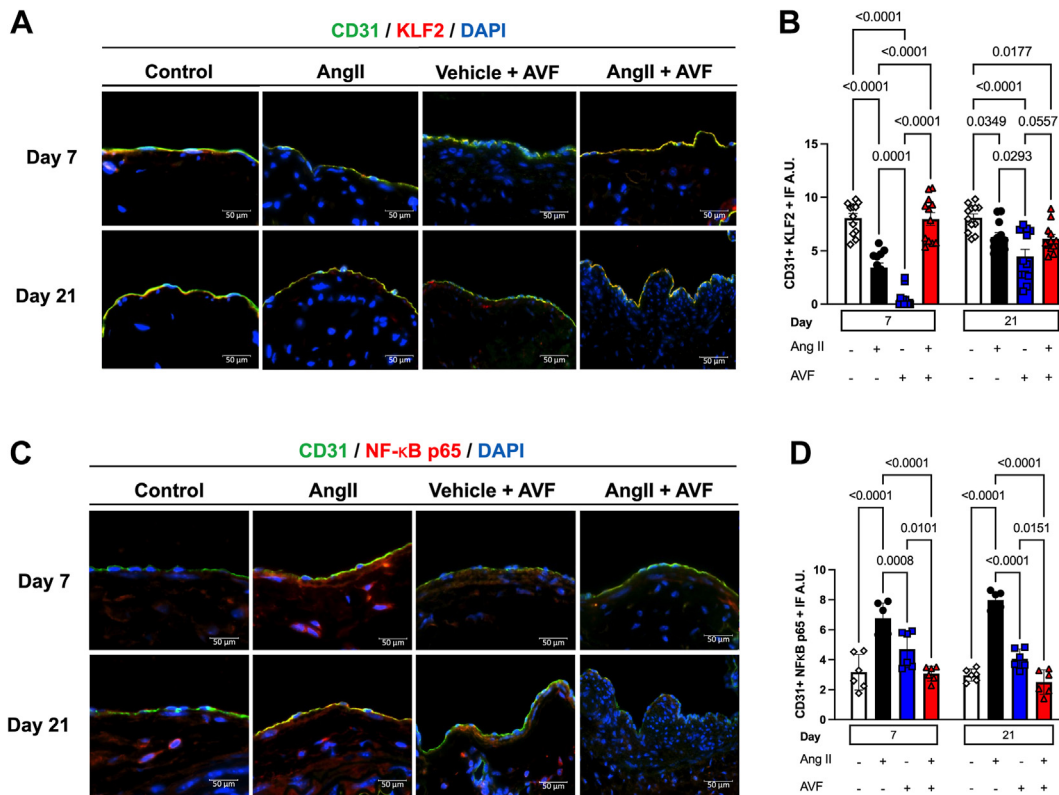


Fig 5. Kruppel-like factor 2 (*KLF2*) and nuclear factor- κ B p65 (*NF- κ B p65*) in the arteriovenous fistula (AVF) without or with hypertension. **A**, Merged immunofluorescence showing CD31 (green), *KLF2* (red), and DAPI (blue) in the control (first column), angiotensin II (*Ang II*) (second column), vehicle + AVF (third column), and *Ang II* + AVF groups (fourth column), at day 7 (first row) or 21 (second row); scale bar, 50 μ m; n = 6. Localization in the nucleus and cytoplasm is expected per the vendor's data (Table). **B**, Bar graph showing mean CD31 + *KLF2* fluorescence intensity; $P \leq .0001$ (two-way analysis of variance [ANOVA]); values of Tukey's multiple comparisons test are shown; n = 12. **C**, Merged immunofluorescence showing CD31 (green), *NF- κ B p65* (red), and DAPI (blue) in the control (first column), *Ang II* (second column), vehicle + AVF (third column), and *Ang II* + AVF groups (fourth column), at day 7 (first row) or 21 (second row); scale bar, 50 μ m; n = 6. Localization in the nucleus and cytoplasm is expected per the vendor's data (Table). **D**, Bar graph showing mean CD31 + *NF- κ B p65* fluorescence intensity; $P \leq .001$ (two-way ANOVA); values of Tukey's multiple comparisons test are shown; n = 6.

geometry of the fistula and hemodynamics are related to AVF remodeling¹⁶; eNOS is a mediator of AVF remodeling.²⁷ In another model of hypertension, eNOS knockout mice had elevated blood pressure but thinner AVF walls compared with control mice, suggesting that different models of hypertension may have different effects on venous remodeling in the fistula environment.³⁶ In the *Ang II* hypertension model, mice with hypertension have increased *KLF2* (Fig 5), perhaps due to less turbulence or increased laminar flow in the outflow vein (Fig 2); our data showing decreased *NF κ B* expression in the hypertensive AVF (Fig 5) is consistent with less turbulent flow. Activation of the *NF κ B* signaling pathway by *Ang II* potentiates target organ damage in hypertension,^{37,38} whereas sustained inhibition of *NF- κ B* prevents hypertension in spontaneously hypertensive rats.³⁹ These results show the importance of the *KLF2* and *NF κ B* pathways, and thus targeting these pathways may be a potential therapeutic strategy to improve AVF patency in patients with hypertension.

This study has several limitations. First, we used an *Ang II* model of hypertension delivered (500 ng/kg/min) continuously through a subcutaneous osmotic pump, and examination of different *Ang II* doses could establish differing effects on venous remodeling. Similar to the experience from other groups with *Ang II*, we noted a steady increase in blood pressure up to 4 weeks from implantation of the *Ang II* Azlet pump.⁴⁰ Although there is some variability in plateauing of blood pressure, this is likely due to measurement techniques and variability in dosage.^{41,42} Also, the hemodynamic measurements were performed with a non-invasive cuff, allowing serial examinations, but may not correlate with central invasive measurements. Notably, given that the tail artery branch is caudal to the aortocaval fistula, future correlation with invasive central blood pressure measurements will help better characterize these hemodynamic changes. We also did not assess the effect of altering the function of the *Ang II* receptor, nor of the downstream components

of the KLF2 or NFκB pathways. Last, because AVF patency is reduced in female mice using this model,⁸ we did not evaluate for sex differences in this study.

CONCLUSION

In conclusion, a central aortocaval AVF decreases systemic hypertension in hypertensive mice, similar to recent human studies using an iliac AVF. However, the effects of hypertension on venous remodeling may influence fistula maturation and long-term patency, and thus additional studies examining the effects of the AVF in the chronic kidney disease environment are warranted.

AUTHOR CONTRIBUTIONS

Conception and design: AB, HL, AD

Analysis and interpretation: AB, RA, HL, LG, YA, YO, JL, CT, RT, WZ, HB, BY, AD

Data collection: AB, RA, HL, HB, AD

Writing the article: AB, RA, HB, AD

Critical revision of the article: AB, RA, HL, LG, YA, YO, JL, CT, RT, WZ, HB, BY, AD

Final approval of the article: AB, RA, HL, LG, YA, YO, JL, CT, RT, WZ, HB, BY, AD

Statistical analysis: AB, RA

Obtained funding: Not applicable

Overall responsibility: AD

DISCLOSURES

None.

REFERENCES

- Singh S, Shankar R, Singh GP. Prevalence and associated risk factors of hypertension: a cross-sectional study in urban varanasi. *Int J Hypertens*. 2017;2017:5491838.
- Unger T, Borghi C, Charchar F, et al. International society of hypertension global hypertension practice guidelines. *Hypertension*. 2020;75:1334–1357.
- Frohlich ED. Hypertension: our major challenges. *Hypertension*. 2001;38:990–991.
- Ott C, Lobo MD, Sobotka PA, et al. Effect of arteriovenous anastomosis on blood pressure reduction in patients with isolated systolic hypertension compared with combined hypertension. *J Am Heart Assoc*. 2016;5:e004234.
- Lobo MD, Ott C, Sobotka PA, et al. Central iliac arteriovenous anastomosis for uncontrolled hypertension: one-year results from the ROX CONTROL HTN trial. *Hypertension*. 2017;70:1099–1105.
- Foran JP, Jain AK, Casserly IP, et al. The ROX coupler: creation of a fixed iliac arteriovenous anastomosis for the treatment of uncontrolled systemic arterial hypertension, exploiting the physical properties of the arterial vasculature. *Catheter Cardiovasc Interv*. 2015;85:880–886.
- Lobo MD, Sobotka PA, Stanton A, et al. Central arteriovenous anastomosis for the treatment of patients with uncontrolled hypertension (the ROX CONTROL HTN study): a randomised controlled trial. *Lancet*. 2015;385:1634–1641.
- Kudze T, Ono S, Fereydooni A, et al. Altered hemodynamics during arteriovenous fistula remodeling leads to reduced fistula patency in female mice. *JVS Vasc Sci*. 2020;1:42–56.
- Yamamoto K, Li X, Shu C, Miyata T, Dardik A. Technical aspects of the mouse aortocaval fistula. *J Vis Exp*. 2013;77:e50449.
- Yamamoto K, Protack CD, Tsuneki M, et al. The mouse aortocaval fistula recapitulates human arteriovenous fistula maturation. *Am J Physiol Heart Circ Physiol*. 2013;305:H1718–H1725.
- Intengan HD, Schiffrin EL. Vascular remodeling in hypertension: roles of apoptosis, inflammation, and fibrosis. *Hypertension*. 2001;38:581–587.
- Lu H, Howatt DA, Balakrishnan A, et al. Subcutaneous angiotensin II infusion using osmotic pumps induces aortic aneurysms in mice. *J Vis Exp*. 2015;103:53191.
- Taniguchi R, Ono S, Isaji T, et al. A mouse model of stenosis distal to an arteriovenous fistula recapitulates human central venous stenosis. *JVS-Vascular Science*. 2020;1:109–122.
- Xue B, Johnson AK, Hay M. Sex differences in angiotensin II-induced hypertension. *Braz J Med Biol Res*. 2007;40:727–734.
- Wilde E, Aubdool AA, Thakore P, et al. Tail-cuff technique and its influence on central blood pressure in the mouse. *J Am Heart Assoc*. 2017;6:e005204.
- Bai H, Sadaghianloo N, Gorecka J, et al. Artery to vein configuration of arteriovenous fistula improves hemodynamics to increase maturation and patency. *Sci Transl Med*. 2020;12:eaax7613.
- Beswick R, Dorrance A, Rajagopalan S, Webb RC. Nf-kb inhibition lowers blood pressure in mineralocorticoid hypertensive rats. *Hypertension*. 2000;36:692.
- Zhao G, Xu MJ, Zhao MM, et al. Activation of nuclear factor-kappa B accelerates vascular calcification by inhibiting ankylosis protein homolog expression. *Kidney Int*. 2012;82:34–44.
- Yamamoto K, Protack C, Kuwahara G, et al. Disturbed shear stress reduces Klf2 expression in arterial-venous fistulae in vivo. *Physiol Rep*. 2015;3:e12348.
- Ewen S, Ukena C, Linz D, et al. Reduced effect of percutaneous renal denervation on blood pressure in patients with isolated systolic hypertension. *Hypertension*. 2015;65:193–199.
- Lee SR, Thorn S, Guerrero N, et al. Arteriovenous fistula-induced cardiac remodeling shows cardioprotective features in mice. *JVS Vasc Sci*. 2021;2:110–128.
- Hadrava V, Kruppa U, Russo RC, Lacourcière Y, Tremblay J, Hamet P. Vascular smooth muscle cell proliferation and its therapeutic modulation in hypertension. *Am Heart J*. 1991;122:1198–1203.
- Hu H, Patel S, Hanisch JJ, et al. Future research directions to improve fistula maturation and reduce access failure. *Semin Vasc Surg*. 2016;29:153–171.
- Deinum J. Collagen and hypertension. *J Hypertens*. 2002;20:1275–1276.
- Querejeta R, López B, González A, et al. Increased collagen type I synthesis in patients with heart failure of hypertensive origin: relation to myocardial fibrosis. *Circulation*. 2004;110:1263–1268.
- Stakos DA, Tziakas DN, Chalikias GK, Mitrousi K, Tsigalou C, Boudoulas H. Associations between collagen synthesis and degradation and aortic function in arterial hypertension. *Am J Hypertens*. 2010;23:488–494.
- Pike D, Shiu YT, Cho YF, et al. The effect of endothelial nitric oxide synthase on the hemodynamics and wall mechanics in murine arteriovenous fistulas. *Sci Rep*. 2019;9:4299.
- Hall MR, Yamamoto K, Protack CD, et al. Temporal regulation of venous extracellular matrix components during arteriovenous fistula maturation. *J Vasc Access*. 2015;16:93–106.
- Woodside KJ, Bell S, Mukhopadhyay P, et al. Arteriovenous fistula maturation in prevalent hemodialysis patients in the United States: a national study. *Am J Kidney Dis*. 2018;71:793–801.
- Eslami MH, Zhu CK, Rybin D, Doros G, Siracuse JJ, Farber A. Simple predictive model of early failure among patients undergoing first-time arteriovenous fistula creation. *Ann Vasc Surg*. 2016;35:46–52.
- Lilly MP, Lynch JR, Wish JB, et al. Prevalence of arteriovenous fistulas in incident hemodialysis patients: correlation with patient factors that may be associated with maturation failure. *Am J Kidney Dis*. 2012;59:541–549.
- Rezapour M, Khavanin Zadeh M, Sepehri MM, Alborzi M. Less primary fistula failure in hypertensive patients. *J Hum Hypertens*. 2018;32:311–318.
- Davies PF, Civelek M, Fang Y, Fleming I. The atherosusceptible endothelium: endothelial phenotypes in complex haemodynamic shear stress regions in vivo. *Cardiovasc Res*. 2013;99:315–327.
- Gimbrone MA Jr, García-Cardena G. Endothelial cell dysfunction and the pathobiology of atherosclerosis. *Circ Res*. 2016;118:620–636.

35. Pober JS, Sessa WC. Evolving functions of endothelial cells in inflammation. *Nat Rev Immunol*. 2007;7:803–815.
36. Hashimoto T, Isaji T, Hu H, et al. Stimulation of caveolin-1 signaling improves arteriovenous fistula patency. *Arterioscler Thromb Vasc Biol*. 2019;39:754–764.
37. Muller DN, Dechend R, Mervaala EM, et al. NF-kappaB inhibition ameliorates angiotensin II-induced inflammatory damage in rats. *Hypertension*. 2000;35:193–201.
38. Crowley SD. Linking angiotensin II to nuclear factor-kappaB light chain enhancer of activated B cells-induced cardiovascular damage: bad CARMAs. *Hypertension*. 2014;64:933–934.
39. Rodríguez-Iturbe B, Ferrebuz A, Vanegas V, Quiroz Y, Mezzano S, Vaziri ND. Early and sustained inhibition of nuclear factor-kappaB prevents hypertension in spontaneously hypertensive rats. *J Pharmacol Exp Ther*. 2005;315:51–57.
40. Gomolak JR, Didion SP. Angiotensin II-induced endothelial dysfunction is temporally linked with increases in interleukin-6 and vascular macrophage accumulation. *Front Physiol*. 2014;5:396.
41. Daugherty A, Manning MW, Fau - Cassis LA, Cassis LA. Angiotensin II promotes atherosclerotic lesions and aneurysms in apolipoprotein E-deficient mice. *J Clin Invest*. 2000;105:1605–1612.
42. Mori K, Okuma H, Nakamura S, et al. Melanocortin-4 receptor in macrophages attenuated angiotensin II-induced abdominal aortic aneurysm in mice. *Sci Rep*. 2023;13:19768.

Submitted Jul 5, 2023; accepted Jan 11, 2024.